# High frequency visual stimulation primes gamma oscillations for visually-evoked phase reset and enhances spatial acuity

Crystal L. Lantz[1*], and Elizabeth M. Quinlan[1,2,3]

[1] Department of Biology, [2]Neuroscience and Cognitive Science Program, [3]Brain and Behavior Institute
University of Maryland; College Park, MD, 20742; USA

* Corresponding Author, clantz@umd.edu





**Abstract**

The temporal frequency of sensory stimulation is a decisive factor in the plasticity of perceptual detection thresholds. However, surprisingly little is known about how distinct temporal parameters of sensory input differentially recruit activity of neuronal circuits in sensory cortices. Here we demonstrate that brief repetitive visual stimulation induces long-term plasticity of visual responses revealed 24 hours after stimulation, and that the location and generalization of visual response plasticity is determined by the temporal frequency of the visual stimulation. Brief repetitive low frequency stimulation (LFS, 2 Hz) is sufficient to induce a visual response potentiation that is expressed exclusively in visual cortex layer 4 and in response to a familiar stimulus. In contrast, brief, repetitive high frequency stimulation (HFS, 20 Hz) is sufficient to induce a visual response potentiation that is expressed in all cortical layers and transfers to novel stimuli. HFS induces a long-term suppression of the activity of fast-spiking interneurons and primes ongoing gamma oscillatory rhythms for phase-reset by subsequent visual stimulation. This novel form of generalized visual response enhancement induced by HFS is paralleled by an increase in visual acuity, measured as improved performance in a visual detection task.

**Keywords:**

Visual Cortex, Plasticity, Oscillations, Photic Tetanus, Mouse

## Introduction

Enduring changes in synaptic strength induced by specific frequencies of afferent stimulation are a primary mechanism for information storage in neural circuits. A wealth of data from brain slices demonstrates that high frequency stimulation rapidly induces long-term potentiation (LTP) of excitatory synapses, while low frequency stimulation induces synaptic long-term depression (LTD; Bliss and Lømo 1973; Dudek and Bear 1992; Kirkwood et al. 1996; Mayford et al. 1995). Repetitive stimulation delivered *in vivo* in animal models mirrors this dependence of bidirectional synaptic plasticity on the stimulation temporal frequency, with synaptic depression and potentiation induced by low and high frequency stimulation respectively (Nabavi et al. 2014; Rodríguez-Durán et al. 2017; O'Riordan et al. 2018). Furthermore, high frequency direct stimulation of the visual thalamus or high frequency photic tetanus induces long lasting enhancement of visual responses (Heynen and Bear 2001; Zhang, Tao, and Poo 2000; Clapp et al. 2006; Teyler et al. 2005; Eckert et al. 2013; Ross et al. 2008; Clapp et al. 2012). Experiments in human subjects utilizing high frequency sensory stimulation also demonstrate rapid enhancement of response amplitudes and lowering of perceptual thresholds in visual, auditory, and somatosensory systems (Beste et al. 2011; Brickwedde et al. 2020; Marzoll et al. 2018; Pegado et al. 2016; Ross et al. 2008; Kirk et al. 2010, Sumner et al. 2020). Enhancement of sensory responses induced by non-invasive sensory stimulation require NMDA receptor activation, sharing the induction

requirements for LTP (Clapp et al. 2006; Dinse et al. 2003). Frequency-dependent changes in neuronal activity and perception are also induced by transcranial stimulation.

Long-lasting enhancement of visual responses that require NMDA receptor activity are also induced in mouse primary visual cortex (V1) following daily repetition of low frequency visual stimulation (LFS; Frenkel et al. 2006). This experience-dependent response plasticity includes an increase in the amplitude of the VEP recorded in layer 4 of V1 and an increase in the peak firing rate of regular-spiking (RS) neurons (Cooke et al. 2015). Response potentiation induced by daily LFS is highly selective for the orientation, contrast and spatial frequency of the visual stimulus used for induction. Indeed, response potentiation is not observed following rotation of the orientation of the visual stimulus by as little as 5 degrees (Cooke and Bear, 2010). The time course and selectivity of visual response potentiation following daily LFS shares many similarities with perceptual learning and LTP, including a requirement for sleep consolidation (Poggio et al. 1992; Zaehle et al. 2007; Aton et al. 2014). Interestingly, the selectivity of daily LFS visual response potentiation is lost following optogenetic suppression of parvalbumin expressing fast spiking interneurons (Kaplan et al. 2016). A reduction in putative fast spiking interneuron (FS IN) excitability following deletion of the AMPAR-binding protein neuronal pentraxin 2 (NPTX2; aka NARP), which is highly enriched at excitatory synapses onto FS INs, inhibits the induction of visual response potentiation by a single bout of LFS (Chang et al. 2010; Gu et al. 2013; O'Brien et al. 1999; Xu et al. 2003). However, high temporal frequency visual stimulation (HFS, 20 Hz) can rescue visual response potentiation in NPTX2$^{-/-}$ mice (Gu et al. 2013).

Sensory response amplitudes and perceptual detection thresholds reflect the interaction between stimulus-evoked neuronal activity and fluctuations in the cortical local field potential (LFP; Sauseng et al. 2007; Xing et al. 2012). In V1, the power of several bands of oscillatory activity in layer 4 increases in response to a familiar stimulus, suggesting that changes in oscillatory power encode visual stimulus familiarity (Kissinger et al. 2018). In concert, the phase of cortical oscillations regulates response magnitude and perception of incoming visual stimuli (Kim et al. 2007). The temporal frequency of incoming auditory and somatosensory stimulation can also impact sensory perception through entrainment of ongoing cortical oscillations (Brickwedde et al. 2020; ten Oever et al. 2017). Indeed, increased power and synchronization of high frequency cortical oscillations is thought to underlie improvements in stimulus detection and memory encoding by attention and motivation Jutras et al. 2009; Montgomery and Buzsáki, 2007; Lisman, 2010). Thus, changes in the time-locked evoked response, as well as the magnitude and phase of ongoing cortical oscillations, are candidate mechanisms for synaptic plasticity evoked by repetitive sensory stimulation (Brickwedde et al. 2019; Howe et al. 2017; Park et al. 2016).

Although the temporal parameters of visual stimulation play a decisive role in the induction of plasticity of visual responses and perceptual thresholds, it is not known how the temporal frequency of visual stimulation

differentially recruits activity in V1 neuronal circuitry. Here we directly compare the impact of two distinct temporal frequencies of repetitive visual stimulation on long-lasting changes in visual response magnitude and visual acuity in the mouse. We find that a single bout of LFS is sufficient to induce a visual response potentiation that is restricted to visual cortex layer 4 and the familiar visual stimulus. In contrast a single bout of HFS is sufficient to induce visual response potentiation throughout V1 that transfers to novel stimuli. HFS induces a long-lasting suppression of the output of FS INs and sensitizes cortical gamma oscillations to phase reset by all subsequent visual stimuli. This general enhancement of visual response strength following HFS is paralleled by improved visual acuity revealed by performance in a visual detection task.

**Materials and Methods**

*Animals.* Experiments utilized equal numbers of male and female adult (postnatal day 60-90) C57BL/6J mice (Jackson Lab, Bar Harbor, ME). Subjects were housed on a 12:12 hour dark:light cycle with food and water *ad libitum*. Experiments were initiated ~6 hours into the light phase. All procedures conformed to the guidelines of the University of Maryland Institutional Animal Care and Use Committee and in accordance with the guidelines published in the NIH Guide for the Care and Use of Laboratory Animals. Sample sizes were determined by power analysis of previous studies quantifying the effect of visual experience on visual response amplitudes.

*Electrophysiology.* House-made 1.2 mm length 16-channel shank electrodes were implanted into binocular V1 (from Bregma: posterior, 2.8 mm; lateral, 3.0 mm; ventral, 1.2 mm), under anesthesia with 2.5% isoflurane in 100% $O_2$, as described (Bridi et al. 2018; Murase et al. 2017). Multichannel electrode arrays were built as previously described (Zold and Hussain Shuler 2015; Murase et al. 2017). Briefly, platinum iridium wires with a diameter of 15 µm (California Fine Wire) were glued into a flat array and cut at an angle to obtain a spacing of approximately 75 µm. Each electrode tip was electroplated with gold (SIFCO Applied Surface Concepts, Fig S1 A). Subjects received a single dose of carprofen (5 mg/kg, SQ) for post-surgical analgesia after the return of the righting reflex. One week after surgery and one day before electrophysiological recordings, subjects were habituated for 45 minutes to head restraint. Broadband electrophysiological data was collected from awake head-fixed mice, using RZ5 bioamp processor and RA16PA preamp (Tucker Davis Technologies, TDT). Multiunit waveforms were sorted into single units using an automatic Bayesian clustering algorithm in OpenSorter (TDT) as described (Murase et al. 2017). Single units (SUs) were processed in MATLAB and classified as regular spiking neurons (RS, presumptive excitatory) or putative fast spiking interneurons (FS IN, presumptive inhibitory) based on waveform slope 0.5 msec after the trough, time between trough and peak, and the ratio of trough to peak height (Niell and Stryker, 2008, Fig S1 E&F). VEPs and SUs were assigned to cortical layer based on LFP waveform shape, and current source density calculated with single site spacing from the laminar array (Guo et al. 2017; Mitzdorf, 1985, Fig S1 B&C).

*Visual Stimulation.* Visual stimuli were presented to both eyes simultaneously using MATLAB (Mathworks) with Psychtoolbox extensions (Brainard, 1997; Pelli, 1997). Prior to visual stimulation each day mice passively viewed a grey 26 cd/$m^2$ screen for 200 seconds to acquire spontaneous activity. Visually evoked responses were recorded in response to 200 seconds of 0.05 cycles per degree, 100% contrast, square-wave gratings reversing at 2 Hz (LFS). Responses were averaged over 1 second. Subjects received 2 Hz LFS stimulation for the acquisition of baseline, initial VEPs. A subset of subjects then received visual stimulation at 20 Hz (HFS). VEPs were acquired on day 2 in response to 2 Hz stimulation in response to familiar and novel stimulus orientations and compared back to the baseline response to 2 Hz stimulation.

*Data Analysis.* Spike rates of sorted SUs were calculated as the average over each 1 second epoch (200 seconds of continuous visual stimulation). Peristimulus-time histograms (PSTH) were calculated for each SU using 5 ms bins and smoothed with a gaussian kernel (Kissinger et al. 2018). To examine changes in oscillatory power by frequency, PSTHs were z-scored and filtered from 1 to 100 Hz using a sliding frequency window via a bandpass elliptic filter with a span of 3 Hz in MATLAB. The analytic signal of band-passed PSTHs was calculated using a Hilbert transform, and the absolute value was used to calculate power within each frequency band.

Visually evoked potentials (VEPs) were calculated as the trough to peak amplitude of the average of 1 second LFP epochs during visual stimulation in MATLAB, as described (Murase et al. 2017). To examine changes in oscillatory power by frequency and the reliability of incoming visual stimulation to reset the phase of ongoing oscillations (Inter-Trial Phase Consistency, ITPC, a time locked measure of oscillatory phase), spontaneous and evoked LFPs were z-scored then convolved with complex Morlet wavelets from 1 to 100 Hz using a 3 Hz window (Fiebelkorn et al. 2018). The wavelet cycle width varied with filtered frequency (1-10 Hz = 2 cycles, 11-14 Hz = 3 cycles, 15-20 Hz = 4 cycles, 21-100 Hz = 5 cycles). The absolute value of the complex vector was used to calculate oscillatory power. Power was averaged across trials for each subject, and activity is reported as percent change in power relative to spontaneous activity recorded on the first day prior to experimental manipulation (experimental – baseline / baseline x 100). Averaged percent change in evoked power was calculated during the 100-200 ms post stimulus onset, binned oscillatory activity was averaged from this window. Oscillatory bins were defined as: delta 1-4 Hz, theta 4-8 Hz, alpha 8-13 Hz, beta 13-30 Hz, and gamma 30-100 Hz. The second half of the complex vector was normalized, averaged and the absolute value was used to calculate ITPC. ITPC was binned by oscillatory frequency. Utilizing the calculated oscillatory phase of the LFP, the phase of each frequency for each single unit was calculated then averaged as Spike-Phase Consistency.

*Behavior.* Psychophysical measurements of spatial acuity were obtained through with performance in a 2 alternative forced choice visual detection task. Task training and testing utilized a Bussey-Saksida Touch

Screen Chamber (Lafayette Instruments; Horner et al. 2013) with custom plexiglass inserts. An opaque insert divided the LCD touch screen into two vertical halves, for simultaneous display of the correct and incorrect visual stimuli. A transparent plexiglass insert, parallel to and 6cm from the touch screen, with 2 5x7 cm swing-through doors, defined the choice point for the calculation of visual stimulus spatial frequency (Fig 7A). Naïve adult mice were trained to associate a high contrast (100%), low spatial frequency (0.05 cycles/degree), 45° sinusoidal grating (positive stimulus) with positive reinforcement (strawberry milk and tone, 3 kHz, 0.5 secs) and a grey image of equal luminance (32 cd/m2; negative stimulus) with negative reinforcement (tone, 400 Hz, 2 sec). Subjects were food deprived for 20 hours a day, with 4 hours of *ad libitum* food access at the end of each training session. A training session consisted of 30 trials, or 45 minutes. To begin a trial, the subject nose-poked in the illuminated liquid reward tray at the rear of the chamber, to trigger the presentation of positive and negative visual stimuli. Contact with the touch screen turned the visual stimulus off. Choosing the positive stimulus resulted in a liquid reward, choosing the negative stimulus resulted in negative reinforcement and a 30 second timeout period. Trials were separated by a 10 second intertrial interval, followed by illumination of the liquid reward tray to signal the beginning of a new trial. Criterion was defined as 25/30 correct trials within 45 minutes = 83% correct). After reaching criterion, acuity testing was initiated. In acuity testing, the positive stimulus was rotated to a novel orientation (45°+15°). Following successful completion (≥ 70%) of a block of 10 trials, the spatial frequency was increased incrementally (0.05 cpd steps). The highest spatial frequency with performance of ≥ 70% correct choices is defined as spatial acuity. Following assessment of initial acuity subjects were randomly divided into 2 groups, 50% viewed 200 seconds of LFS, 50% viewed 200 seconds of HFS, at a novel orientation, and were returned to their home cage. 24 hours after visual stimulation, acuity was tested at a familiar stimulus orientation (used for LFS or HFS) and at a novel orientation, with test order randomized. Subjects were then returned to food and water *ad libitum* in the mouse colony.

*Statistics.* Statistical analysis was completed using JASP (JASP Stats). Repeated measures ANOVA (RANOVA) was used to compare LFP data from 3 time points within the same subject, including VEP, oscillatory power and ITPC, followed by a Bonferroni *post-hoc* when appropriate. For single unit recordings, we did not assume that we were recording from the same unit over multiple days, therefore, unpaired Student's t-test was used to compare 2 groups and a one-way ANOVA was used to compare 3 groups, followed by a Tukey *post-hoc* when appropriate. A multivariate ANOVA (MANOVA) with a Bonferroni *post-hoc,* when appropriate, was used to compare oscillatory data consisting of 2 time points and multiple frequency bands. To compare the change in oscillatory power within subjects we employed a one-sample Student's t-test with a Bonferroni correction for multiple comparisons. In text, n is reported as the total number of subjects, followed by the total number of single units. Exact p values are reported in the text, except when $p < 0.001$.

**Results**

Plasticity of visual responses is dependent on visual stimulation frequency

To examine the impact of the temporal frequency of repetitive visual stimulation on visual response plasticity, we examined the magnitude of visually-evoked potentials (VEPs) simultaneously in all layers of the primary visual cortex (V1). We focused on the long-term effects of one bout of visual stimulation, as described (Gu et al. 2013; Montey et al. 2013). Head-fixed awake mice viewed 200 seconds of square-wave gratings (0.05 cycles per degrees, 100% contrast, 60° orientation) delivered at low frequency (LFS, 2 Hz) or high frequency (HFS, 20 Hz, Fig. 1 A&C) and VEPs were averaged over 1 second. 24 hours after LFS or HFS VEPs were recorded a second time in response to visual stimulation with a familiar (60°) and novel (150°) orientation. Long lasting visual response potentiation was induced by both protocols, and the location and generalization of visual response potentiation was determined by the stimulus temporal frequency. 24 hours after a single bout of low frequency stimulation (LFS), the amplitude of the layer 4 VEP was significantly increased in response to familiar (60°), but not novel (150°) visual stimulus orientations, mimicking the stimulus selectivity of response potentiation induced by LFS over multiple days (Frenkel et al. 2006; n = 16, $RANOVA_{(df, 2, 15)}$, Bonferroni *post-hoc*, F = 9.13, p < 0.001; initial v. familiar: p = 0.023, Fig. 1 B).

In contrast, 24 hours after a single bout of high frequency stimulation (HFS), VEP amplitudes were significantly increased in all layers of V1 in response to both familiar (60°) and novel (150°) visual stimulus orientations (n=11, $RANOVA_{(df, 2, 10)}$, Bonferroni *post-hoc*, layer 2/3: F = 5.25, p = 0.015, initial v. familiar p = 0.023, initial v novel p = 0.032; layer 4: F = 7.31, p = 0.004, initial v. familiar p = 0.038, initial v. novel: p = 0.005; layer 5/6: F = 11.41, p < 0.001, initial v. familiar: p = 0.005, initial v. novel: p = 0.022, Fig. 1D). 24 hours after HFS, amplitudes evoked by visual stimuli of novel spatial frequencies were also increased (Fig. S2). To control for the delivery of 2 Hz stimulation used for assessment of baseline VEPs prior to delivery of 20 Hz stimulation, we also examined VEP amplitudes in subjects that received 20 Hz stimulation prior to 2 Hz stimulation. Generalized visual response potentiation was observed throughout V1 if HFS (20Hz) stimulation preceded or followed assessment of initial baseline VEP amplitudes (Between subjects $RANOVA_{(df 1,12)}$ layer 2/3: F = 0.001, p = 0.97, layer 4: F = 0.010, p = 0.92, layer 5: F = 0.00003, p = 0.995, data not shown). Notably, we observe no evidence of immediate potentiation of VEPs in response to HFS, as VEP amplitudes acquired with subsequent baseline stimulation (2 Hz) were similar to unstimulated controls (Naive initial: layer 2/3:81.12 ± 11.47 μV; layer 4: 110.02 ± 19.34 μV; layer 5: 80.80 ± 10.92 μV; initial following HFS: layer 2/3:76.66 ± 7.61 μV; layer 4: 115.49 ± 25.12 μV; layer 5: 79.52 ± 17.91 μV. $RANOVA_{(df, 1, 12)}$, Between subjects, F = 0.00012 p = 0.997). HFS and LFS visual stimulation was matched for stimulus duration and not number of stimulus reversals, as previous work demonstrates that repetitive LFS over consecutive day induces stimulus-specificity response potentiation in layer 4 (Cooke and Bear, 2010; Frenkel et al. 2006). Thus, response potentiation induced by a single bout of LFS is localized and stimulus-specific, while HFS induced response potentiation is global and transfers to novel stimuli.

Visual stimulus frequency acutely modulates oscillatory power, phase, and LFP-spike coupling in V1

The VEP amplitude reflects the interaction between stimulus-evoked synaptic potentials and ongoing fluctuations in the cortical local field potential (LFP). Changes in VEP amplitude could therefore reflect changes in the power or phase of LFP oscillations. To ask how the power of LFP oscillations was impacted during LFS and HFS, we normalized the absolute value of the complex Morlet wavelet convolved LFP during visual stimulation to pre-stimulation spontaneous activity (equal luminance grey screen; 26 cd/m$^2$). LFS and HFS induced similar changes in LFP oscillatory power. During LFS, low frequency (alpha and beta bands) LFP oscillatory power increased significantly in all cortical layers (n = 16, one-sample t-test. Layer 2/3: α: t = 4.44, p < 0.001, β: t = 4,39, p < 0.001. Layer 4: α: t = 2.37, p = 0.015, β: t = 2.31, p = 0.024. Layer 5: α: t = 4.07, p < 0.001, β: t = 2.27, p = 0.019, Fig. 2 A, S3 A&B). During HFS, low frequency (delta, alpha and beta bands) power increased significantly in all layers (n=11, one-sample t-test, layer 2/3; δ: t = 2.42, p = 0.019, α: t = 3.21, p = 0.005, beta, t = 3.57, p = 0.003; layer 4; δ: t = 2.11, p = 0.031, α: t = 2.94, p = 0.008, β: t = 2.82, p = 0.009; layer 5; δ: t = 2.31, p = 0.023, α: t = 1.93, p = 0.042, β: t = 1.92, p = 0.043; Fig. 2 C, S3 C&D).

To ask how the temporal frequency of visual stimulation impacted the phase of ongoing LFP oscillations, we convolved the LFP signal with a complex Morlet wavelet and calculated the angle of the resultant complex output. Inter-trial phase consistency (ITPC), which ranges from 0 (if phase was random, and not reset by incoming visual input) and 1 (if phase was reset similarly in all trials), was calculated from the time-locked phase and compared to the ITPC during pre-stimulation spontaneous activity. LFS and HFS had differential effects on the phase reset of ongoing LFP oscillations. LFS increased phase reset for low frequency oscillations (delta, theta, alpha, and beta) in all cortical layers and increased gamma phase reset in layer 2/3 (n = 16 subjects, Layer 2/3: MANOVA $_{(df, 1, 5)}$ F = 15.94, p < 0.001, δ: F = 36.41, p < 0.001, θ: F = 75.21, p < 0.001, α: F = 88.20, p < 0.001, β: F = 42.22, p < 0.001, γ: F = 4.277, p = 0.047. Layer 4: MANOVA $_{(df, 1, 5)}$ F = 15.98, p < 0.001, δ: F = 45.01, p < 0.001, θ: F = 56.15, p < 0.001, α: F = 65.05, p < 0.001, β: F = 39.86, p < 0.001. Layer 5/6: MANOVA $_{(df, 1, 5)}$ F = 11.10, p < 0.001, δ: F = 20.59, p < 0.001, θ: F = 51.07, p < 0.001, α: F = 46.05, p < 0.001, β: F = 35.09, p < 0.001; Fig. 2 B). In contrast, HFS significantly increased phase reset of intermediate frequencies (alpha and beta) in all cortical layers, and increased gamma reset in layers 2/3 and 4. Interestingly, HFS decreased delta reset in all cortical layers, with no changes observed in the phase of theta oscillations (n = 11 subjects, Layer 2/3: MANOVA $_{(df, 1, 5)}$ F = 10.46, p < 0.001, δ: F = 7.76, p = 0.011, α: F = 16.68, p < 0.001, β: F = 43.33, p < 0.001, γ: F = 10.63, p = 0.004. Layer 4: MANOVA $_{(df, 1, 5)}$ F = 11.26, p < 0.001, δ: F = 10.09, p = 0.005, α: F = 28.28, p < 0.001, β: F = 48.15, p < 0.001, γ: F = 5.60, p = 0.028. Layer 5/6: MANOVA $_{(df, 1, 5)}$ F = 6.46, p = 0.002, δ: F = 5.84, p = 0.025, α: F = 24.25, p < 0.001, β: F = 34.24, p < 0.001; Fig. 2 D). The output of putative fast spiking cortical interneurons (FS INs) can regulate LFP amplitudes by influencing the generation of theta rhythms and the power and synchrony of gamma rhythmicity (Cardin et al. 2009; Sohal et al. 2009; Stark et al. 2013). To quantify the pattern and strength of the spiking output of individual FS INs during LFS and HFS we calculated the oscillatory power of the post-stimulus time histogram

from single unit activity. Oscillatory power during visual stimulation was normalized to pre-stimulation spontaneous activity. The temporal frequency of the visual stimulus was reflected in the output of FS INs, as LFS increased the power of low (4 - 8 Hz) as well as mid-frequency oscillations (7 - 30 Hz, n = 16 subjects, 23 units. One-sided t-test, θ: t = 2.22, p = 0.016, α: t = 2.04, p = 0.024, β: t = 1.84, p = 0.036; Fig. 3 A&B). In contrast, HFS increased the power of higher frequency oscillations (13 - 30 Hz, n = 11 subjects, 19 units. One-sided t-test, α: t = 1.81, p = 0.039, β: t = 2.41, p = 0.011; Fig. 3 E&F). To quantify the coherence of FS IN activity with on-going LFP oscillations, we utilized the time-locked LFP phase to calculate the consistency of FS IN spiking within each oscillatory frequency band during LFS and HFS. LFS significantly increased FS IN firing phase consistency with delta oscillations in all cortical layers and theta oscillations in layers 2/3 and 4 (Student's t-test, n = 16 subjects, 22 units, layer 2/3: δ: t = 3.63, p < 0.001, θ: t = 3.66, p < 0.001, layer 4: δ: t = 8.10, p < 0.001, θ: t = 3.87, p < 0.001 layer 5: δ: t = 2.02, p = 0.025, Fig. 3 C&D). Unexpectedly, no significant differences in FS IN firing phase consistency were observed during HFS (Fig. 3 G&H).

Changes in oscillatory power do not predict visual response potentiation

To ask if LFS and HFS induce long-lasting changes in LFP oscillations, we examined the power of spontaneous oscillations and the response to the familiar (60° orientation) and novel (150° orientation) visual stimuli 24 hours after repetitive visual stimulation. We utilized the absolute value of the Morlet wavelet convolved LFP in the time window of maximal visually evoked activity (100 - 200 ms after stimulus reversal). 24 hours after HFS, delta and theta power of spontaneous activity were significantly decreased, (Fig. S4 D&E, S5 B), with no change in spontaneous power 24 hours after LFS (Fig. S4 A&B, S5 A). Thus, HFS induced long-lasting changes in ongoing cortical rhythms.

Visually-evoked changes in LFP power were also different following LFS and HFS. 24 hours after LFS, presentation of visual stimuli with familiar, but not novel orientations significantly increased beta power (13 – 30 Hz) in layers 4 and 5/6 (n = 16, RANOVA $_{(df, 2, 15)}$, Bonferroni *post hoc*. Layer 4: F = 6.51, p = 0.004, initial v. familiar, p = 0.004. Layer 5/6: F = 3.92, p = 0.031, initial v. familiar: p = 0.027; Fig. 4 A&B). In contrast, 24 hours after HFS, presentation of visual stimuli with familiar or novel orientations significantly decreased theta power in all cortical layers (n = 11, RANOVA $_{(df, 2, 10)}$ with Bonferroni *post-hoc*. Layer 2/3: F = 8.633, p = 0.002; initial v. familiar, p = 0.015, initial v. novel, p=0.003. Layer 4: F = 8.47, p = 0.002; initial v. familiar, p = 0.016, initial v. novel, p = 0.003. Layer 5/6: F = 7.936, p = 0.003, initial v. familiar, p=0.018; initial v. novel, p = 0.004, Fig. 4 C&D). Additionally, presentation of novel or familiar visual stimuli 24 hours after HFS significantly decreased delta power in layers 4 and 5/6 (n = 11, RANOVA $_{(df, 2, 10)}$ with Bonferroni *post-hoc*. Layer 4: F= 10.24, p < 0.001; initial v familiar, p = 0.031, initial v. novel, p < 0.001. Layer 5/6: F = 7.681, p = 0.003, initial v familiar, p = 0.04, initial v novel, p = 0.003, Fig. 4D).

Visually-evoked reset of ongoing gamma oscillations predicts visual response potentiation

The phase of on-going LFP oscillations, and the ability to reset phase with visual stimulation, can modify the amplitude of visually-evoked responses. To ask if visual response potentiation is coincident with visually-induced phase reset of the LFP we calculated the average ITPC during maximum visually-evoked activity (100-200 ms after stimulus onset). 24 hours after LFS, the familiar visual stimulus significantly increased beta and gamma ITPC specifically in layer 4 (n = 16 subjects. RANOVA $_{(df, 2, 15)}$, Bonferroni *post-hoc*, β: F = 5.20, p = 0.011; initial v. familiar: p = 0.045, γ: F = 8.82, p < 0.001; initial v. familiar: p = 0.005, Fig. 5 A&B). In contrast, 24 hours after HFS, visual stimuli with both familiar and novel orientations significantly increased gamma ITPC in all cortical layers (n = 11 subjects. RANOVA $_{(df, 2, 10)}$, Bonferroni *post-hoc*, layer 2/3: F = 19.42, p < 0.001; initial v. familiar: p = 0.001; initial v. novel: p = 0.003. Layer 4: F = 13.04, p < 0.001; initial v. familiar: p = 0.010; initial v. novel: p = 0.006. Layer 5: F = 5.29, p = 0.025; initial v. familiar: p = 0.022; initial v. novel: p = 0.021, Fig. 5 C&D). Notably, the expression of increased gamma ITCP mirrored the locus and specificity of VEP potentiation following LFS and HFS.

To ask if changes in FS IN activity reflect plasticity of visual responses, we examined the spontaneous spike rate and oscillatory power, and evoked spike rate and oscillatory power in response to visual stimuli with familiar (60°) and novel (150°) orientations 24 hours after LFS or HFS. Spontaneous FS IN firing rate and oscillatory power were suppressed 24 hours after HFS (Fig. S4 F), but unchanged following LFS (Fig. S4 C). Similarly, there were no significant differences in visually-evoked FS IN firing rate or power following LFS (n = 16 subjects, 22 (initial), 23 (familiar), 20 (novel) units; Fig. 6 A&B). However, subsequent visual stimulation in subjects that received HFS significantly suppressed FS IN firing rates and significantly decreased the power of FS output at frequencies above theta (7 - 100Hz; n=11 subjects, 19 (initial), 20 (familiar), 20 (novel) units; firing rates: One-way ANOVA $_{(df, 2, 57)}$, Tukey *post-hoc*, F = 4.50, p = 0.015; initial v. familiar: p = 0.022; initial v. novel: p = 0.046. Fig. 6 E; power: One-way ANOVA $_{(df, 2, 57)}$, Bonferroni *post-hoc*, α: F = 6.862, p = 0.002, initial v. familiar, p = 0.004, initial v. novel, p = 0.011, β: F = 8.898, p < 0.001, initial v. familiar, p = 0.003, initial v. novel, p = 0.001, γ: F = 5.998, p = 0.004, initial v. familiar, p = 0.009, initial v. novel, p = 0.015; Fig. 6 F). We observed no change in the spontaneous spike rates of RS neurons 24 hours after LFS, and a significant increase in visually-evoked RS spiking in layer 4 in response to the familiar orientation, as previously reported (Aton et al. 2014, n = 16 subjects, 33 (initial), 28 (familiar), 25 (novel) units: One-way ANOVA$_{(df, 2, 83)}$ Tukey post-hoc, F = 3.16, p = 0.047; initial v. familiar, p = 0.037, data not shown). 24 hours after HFS, RS units in layer 5 demonstrated a significant decrease in spontaneous firing rates (n = 11 subjects, 20 (0 hours), 15 (24 hours) units. Student's t-test, t = 2.63, p = 0.0065) and evoked firing rates to familiar and novel orientations (n = 11 subjects, 20 (initial), 17 (familiar), 20 (novel) units: One-way ANOVA$_{(df, 2, 54)}$,Tukey post-hoc, F= 6.24, p = 0.0036; initial v. familiar p = 0.014, initial v. novel p = 0.007, data not shown).

To ask how visually-evoked changes in FS IN firing are related to the phase of ongoing LFP oscillatory activity, we calculated spike-phase consistency between each FS IN and the LFP of each cortical layer. 24 hours after

LFS there was no significant change in FS IN spike-LFP-phase consistency in any cortical layer in response to novel or familiar visual stimuli (n = 16 subjects, 22 (initial), 23 (familiar), 20 (novel) units; Fig. 6 C&D). In contrast, 24 hours after HFS, visual stimuli with familiar and novel orientations significantly increased FS IN spike-LFP phase coupling with gamma oscillations across all cortical layers (n = 11 subjects, 19 (initial), 20 (familiar), 20 (novel) units. One-way ANOVA$_{(df, 2, 56)}$, Bonferroni *post-hoc*. Layer 2/3: F = 6.795, p = 0.002, initial v. familiar p = 0.009, initial v. novel p = 0.005. Layer 4: F = 5.655, p = 0.033, initial v. familiar p = 0.008, initial v. novel p = 0.005. Layer 5: F = 6.072, p = 0.004, initial v. familiar p = 0.026, initial v. novel p = 0.006; Fig. 6 G&H). Thus, visual stimulation subsequent to HFS decreases FS IN firing rates, and increases FS IN phase coupling with gamma, throughout the primary visual cortex.

HFS enhances visual acuity

Following HFS, an increase in VEP magnitudes and ITPC is observed in response to visual stimuli with novel orientations and spatial frequencies suggesting that HFS may generally enhance visual acuity. To test this prediction, we examined the impact of LFS and HFS on spatial acuity assessed by performance in a 2 alternative forced-choice spatial frequency detection task utilizing a touchscreen Bussey chamber with a plexiglass insert to define the choice point for calculation of the visual stimulus spatial frequency. Naïve mice (n = 12) were trained to associate a liquid reward with a simple visual stimulus (high contrast (100%), low spatial frequency (0.05 cpd) 45° sinusoidal grating; Fig. 7 A). Subjects performed 30 trials per day, requiring 12.3 ± 1.05 days to reach the criterion of 25/30 correct trials (83%; Fig. 7 B). To assess spatial acuity, the positive stimulus was rotated to a novel orientation (45°±15°), and subjects completed blocks of 10 trials with spatial frequencies from 0.05 cpd to 0.7 cpd in increments of 0.05 cpd. Spatial acuity was defined as highest spatial frequency with performance of ≥ 70% correct choices.

Following determination of baseline spatial acuity, subjects passively viewed 200 seconds of either LFS or HFS at a novel orientation (45° ± 30°). There was no significant difference in baseline spatial acuity between subjects assigned to LFS and HFS groups (average +/- SEM cpd, LFS; 0.33 ± 0.02; HFS 0.30 ± 0.03 cpd, Student's t-test, p = 0.63,Fig. 6 C). 24 hours following visual stimulation, visual performance was assessed at the familiar (45° ± 30°) or another novel orientation (45° ± 60°). Following LFS, we observed no change in spatial acuity assessed with the familiar (0.30 ± 0.03 cpd) or novel visual stimulus (0.37 ± 0.03 cpd; n = 12, RANOVA $_{(df, 2, 11)}$, F = 4.02, p = 0.032, initial v familiar p = 0.303, initial v. novel p = 0.303; Fig. 7 D&E). In contrast, 24 hours after HFS, spatial acuity was significantly enhanced in response to familiar (0.46 ± 0.03 cpd) and novel visual stimulus orientations (0.46 ± 0.03; n = 12, RANOVA $_{(df, 2, 11)}$, Bonferroni *post-hoc*, F = 6.87, p = 0.005; initial v. familiar, p = 0.011; initial v. novel, p = 0.011; Fig. 7 F&G). Together this suggests that HFS induces a sustained, and highly generalizable enhancement of visual function.

**Discussion**

We delineate distinct cellular, circuit, and perceptual consequences of high (HFS) and low (LFS) frequency repetitive visual stimulation in the mouse. A single, short bout of LFS was sufficient to engage selective response potentiation of layer 4 VEPs, that mirrored stimulus-selective response potentiation induced by daily LFS in specificity, locus of expression and the absence of change in FS IN output (Frenkel et al. 2006, Aton et al. 2014). In contrast, a single bout of HFS induced a long-lasting suppression of the output of FS INs, and primed high frequency (gamma) LFP oscillations for subsequent visually-evoked phase reset. Accordingly, we show that subsequent to HFS, VEP amplitudes are potentiated in all layers of V1, and in response to both familiar and novel visual stimuli. Together this demonstrates that the temporal characteristics of repetitive visual stimulation is a decisive factor in the locus of expression and the specificity of visual response plasticity.

It is increasingly appreciated that activity in V1 neurons reflects more than visual input. Indeed, neuronal activity patterns are altered by locomotion (Niell and Stryker, 2010), generalized motor movements, arousal state (Stringer et al. 2019) and input from other sensory systems (Iurilli et al. 2012). Similarly, ongoing cortical rhythms in V1, including beta (12 - 30 Hz) and gamma (30 - 100 Hz), are regulated by visual stimulus parameters including contrast intensity (Saleem et al. 2017) and visual stimulus size (Veit et al. 2017). High frequency and low frequency sensory stimulation can acutely impact discrimination thresholds and induce acute desynchronization of alpha oscillations that last for up to 1 hour (Clapp, 2006). Importantly, changes in cortical oscillatory power induced by bouts of visual stimulation across days encode complex temporal sequences (Gavornik and Bear 2014; Han et al. 2008) and reward timing (Zold and Hussain Shuler, 2015). Similarly, visual stimulus familiarity is encoded by an increase in the visually-evoked power of theta (4 - 8 Hz), alpha (8 - 12 Hz) and beta (12 - 30 Hz) oscillations in V1 layer 4 of V1 (Kissinger et al. 2018; Kissinger et al. 2020). Similarly, we observed an increase in mid-range (alpha and beta) oscillatory activity in V1 in response to a familiar visual stimulus just 24 hours after a single bout of LFS. However, 24 hours after a single bout of HFS, low-range (theta) power was decreased in all cortical layers in response to both familiar and novel visual stimuli. The latter is consistent with our observation that HFS suppresses the firing rate of FS INs, as FS INs have been shown to drive the production of theta oscillations within the cortex and hippocampus (Buzsáki, 2002; Stark et al. 2013). 24 hours after HFS we also observe a decrease in visually-evoked and spontaneous low frequency power (1 – 8 Hz) in all cortical layers in response to novel and familiar stimuli, as seen during directed attention (Schroeder and Lakatos, 2009). Thus LFS and HFS have distinct long-term consequences on LFP oscillatory activity in V1.

Changes in the power of cortical oscillations in the absence of synchronization of oscillatory phase could reduce response magnitude by increasing variability. In contrast, phase synchronization with incoming stimulation could increase response magnitude and decrease response variability. Indeed, co-incident visually-induced phase reset of cortical gamma oscillations predicted both the location and specificity of visual

response potentiation in response to LFS and HFS: both familiar and novel visual stimuli, subsequent to HFS, reset the phase of ongoing gamma oscillations throughout V1, while visually-induced gamma phase reset following LFS is selective for layer 4 and the familiar visual stimulus. The ability to prime high frequency oscillatory activity likely reflects the origins of generation and modulation of gamma oscillations. Cortical gamma oscillations are generated by feedforward thalamo-cortical connections, while phase synchrony is modulated/ entrained by the output of cortical parvalbumin expressing FS INs (Saleem et al. 2017; Cardin et al. 2009; Chen et al. 2017). HFS-induced suppression of FS INs would reduce the impact of cortical activity on gamma synchrony and enhance sensitivity to gamma phase reset by subsequent visually-evoked feed-forward activity. Accordingly, the non-selective response potentiation we observe following HFS is reminiscent of the enhancement of visually evoked responses to both familiar and novel visual stimuli following optogenetic suppression of FS IN output (Kaplan et al. 2016).

LFS and HFS are also likely to recruit activity in different subsets of neurons in mouse V1, tuned to lower and higher temporal frequencies respectively (Gao et al. 2010). Nevertheless, the temporal frequency of the initial visual stimulation was reflected in changes in LFP oscillatory power, phase reset, and FS IN output. The temporal frequency of the HFS used here (20 Hz) is close to flicker fusion in the murine visual system, and may therefore drive the largest number of pyramidal neurons to spike at high frequency (Durand et al. 2016; Tanimoto et al. 2015). Interestingly, the suppression of FS IN firing rates and changes in synchrony of FS IN spiking with oscillations are observed 24 hours after HFS but not during HFS. One likely possibility is that sleep is required to consolidate changes in cortical activity induced by HFS, as has been shown for the stimulus-selective response potentiation induced by daily LFS (Aton et al. 2014).

Our results suggest that the expression site and generalizability of response potentiation are determined by the temporal frequency of the inducing stimulus. The LFS and HFS stimulation protocols used here were matched for total duration, as such HFS subjects received more contrast reversals than those that received LFS. Although we cannot rule out the possibility that the difference in the number of stimulus presentations, and not the temporal frequency of the visual stimulus, underlies the response potentiation following HFS, previous studies have shown that daily repetition of LFS induces a robust response potentiation that is stimulus-specific and expressed in layer 4 (Cooke and Bear, 2010; Frenkel et al. 2006). This suggests that increasing the number of LFS stimulus presentations would not impact the locus or specificity of response potentiation. Yet, the response potentiation induced by our truncated LFS paradigm mirrored the response to daily LFS in specificity and locus of expression, but was more modest in amplitude. It is worth noting that although our initial VEP amplitudes were low compared to previous work utilizing single tungsten electrodes in layer 4 (Frenkel et al. 2006), they are consistent with our previous work utilizing a laminar array of small diameter platinum iridium wires (Murase et al. 2017). Additionally, we cannot rule out the possibility that the synaptic changes underlying improved spatial acuity following HFS reflect plasticity beyond V1, such as the latero-intermediate area, where

neurons are tuned to higher temporal and spatial frequencies than V1 (Marshel et al. 2011). However, perceptual habituation induced by daily LFS transfers from training to testing environments and shares the stimulus selectivity and dependence on NMDARs located in V1 NMDARs (Cooke et al. 2015). Our visual acuity measures are the first to utilize a modified Bussey Chamber (Horner et al. 2013) to which we added a plexiglass swing-through door to identify a choice point for visual stimulus spatial frequency calculation. Our acuity measurements are lower than those previously reported using a water-based task (Prusky et al. 2000) and may reflect the rapid acquisition of the touchscreen visual detection task with a minimal number of trials, or that spatial frequency detection is occurring prior to the arrival at the plexiglass threshold. Nonetheless, our acuity measures are highly consistent within subjects, and only subjects that received HFS stimulation demonstrated improved visual detection.

Our findings provide mechanistic insight into the distinct cellular, circuit and perceptual response to high (HFS) and low (LFS) frequency repetitive visual stimulation, which may lend insight to other forms of sensory system plasticity and to other species. Indeed, cortical oscillations, as well as their functions, are highly conserved across species within multiple spatiotemporal scales, remaining consistent even with increasing brain size (Buzsáki et al. 2013). In humans, a high frequency (20 Hz) luminance flicker induces a long-lasting improvement in luminance change detection, while a low frequency (1 Hz) luminance flicker briefly reduces performance (Beste et al. 2011). Similarly, high frequency (20Hz), but not low frequency (1 Hz), presentation of an oriented bar or a flickering sinusoidal grating improves orientation discrimination (Marzoll et al. 2018). However, the optimal frequency of stimulation to improve visual function may not be consistent across species. Indeed, visual stimulation with a 9 Hz tetanus in humans improves detection thresholds but fails to potentiate VEP amplitudes in rodents (Teyler et al. 2005; Clapp et al. 2012; Eckert et al. 2013; but see Abuleil et al. 2019). Performance on sensory and memory tasks are also manipulated by trans-cranial brain stimulation techniques. Low frequency rTMS (1-3 Hz pulses) stimulation over the visual cortex in cats induced transient depression of the amplitude of visual response amplitudes, while high frequency stimulation (10 Hz) transiently potentiated visual responses (Aydin-Abidin et al. 2006). Together this supports the continued evaluation of HFS visual stimulation for non-invasive vision therapy to promote long-lasting and generalizable enhancement of visual function.

**Acknowledgements**

This work was supported by the National Institutes of Health grant EY016431 and EY025922 to EMQ.

**References**

Abuleil D, McCulloch DL, Thompson B. 2019. Older Adults Exhibit Greater Visual Cortex Inhibition and Reduced Visual Cortex Plasticity Compared to Younger Adults. Front Neurosci. 13:607.

Aton SJ, Suresh A, Broussard C, Frank MG. 2014. Sleep Promotes Cortical Response Potentiation Following Visual Experience. Sleep *37*, 1163–1170.

Aydin-Abidin S, Moliadze V, Eysel UT, Funke K. 2006. Effects of repetitive TMS on visually evoked potentials and EEG in the anaesthetized cat: dependence on stimulus frequency and train duration. J. Physiol. *574*, 443–455.

Beste C, Wascher E, Güntürkün O, Dinse HR. 2011. Improvement and Impairment of Visually Guided Behavior through LTP- and LTD-like Exposure-Based Visual Learning. Curr. Biol. *21*, 876–882.

Bliss TVP, Lømo T. 1973. Long-lasting potentiation of synaptic transmission in the dentate area of the anaesthetized rabbit following stimulation of the perforant path. J. Physiol. 232, 331–356.

Brainard DH. 1997. The Psychophysics Toolbox. Spat. Vis. *10*, 433–436.

Brickwedde M, Krüger MC, Dinse HR. 2019. Somatosensory alpha oscillations gate perceptual learning efficiency. Nat. Commun. *10*, 263.

Brickwedde M, Schmidt MD, Krüger MC, Dinse HR. 2020. 20 Hz Steady-State Response in Somatosensory Cortex During Induction of Tactile Perceptual Learning Through LTP-Like Sensory Stimulation. Front. Hum. Neurosci. *14*, 257.

Bridi MCD, de Pasquale R, Lantz CL, Gu Y, Borrell A, Choi S-Y, He K, Tran T, Hong SZ, Dykman A, Lee H-K, Quinlan EM, Kirkwood A. 2018. Two distinct mechanisms for experience-dependent homeostasis. Nat. Neurosci. *21*, 1.

Buzsáki G. 2002. Theta oscillations in the hippocampus. Neuron *33*, 325–340.

Buzsáki G, Logothetis N, Singer W. 2013. Scaling brain size, keeping timing: Evolutionary preservation of brain rhythms. Neuron.

Cardin JA, Carlén M, Meletis K, Knoblich U, Zhang F, Deisseroth K, Tsai L-H, Moore CI. 2009. Driving fast-spiking cells induces gamma rhythm and controls sensory responses. Nature *459*, 663–667.

Chang MC, Park JM, Pelkey KA, Grabenstatter HL, Xu D, Linden DJ, Sutula TP, McBain CJ, Worley PF. 2010. Narp regulates homeostatic scaling of excitatory synapses on parvalbumin-expressing interneurons. Nat. Neurosci. *13*, 1090–1097.

Chen G, Zhang Y, Li X, Zhao X, Ye Q, Lin Y, Tao HW, Rasch MJ, Zhang X. 2017. Distinct Inhibitory Circuits Orchestrate Cortical beta and gamma Band Oscillations. Neuron *96*, 1403-1418.e6.

Clapp WC, Eckert MJ, Teyler TJ, Abraham, WC 2006. Rapid visual stimulation induces N-methyl-D-aspartate receptor-dependent sensory long-term potentiation in the rat cortex. Neuroreport *17*, 511–515.

Clapp WC, Hamm JP, Kirk IJ, Teyler TJ. 2012. Translating long-term potentiation from animals to humans: A novel method for noninvasive assessment of cortical plasticity. Biol Psychiatry.

Cooke SF, Bear MF. 2010. Visual experience induces long-term potentiation in the primary visual cortex. J. Neurosci. *30*, 16304–16313.

Cooke SF, Komorowski RW, Kaplan ES, Gavornik JP, Bear MF. 2015. Visual recognition memory, manifested as long-term habituation, requires synaptic plasticity in V1. Nat. Neurosci. *18*, 262–271.

Dinse HR, Ragert P, Pleger B, Schwenkreis P, Tegenthoff M. 2003. Pharmacological modulation of perceptual learning and associated cortical reorganization. Science *301*, 91–94.

Dudek SM, Bear MF. 1992. Homosynaptic long-term depression in area CA1 of hippocampus and effects of N-methyl-D-aspartate receptor blockade. Proc. Natl. Acad. Sci. U. S. A. 89, 4363–4367.

Durand S, Iyer R, Mizuseki K, De Vries S, Mihalas S, Reid RC. 2016. A comparison of visual response properties in the lateral geniculate nucleus and primary visual cortex of awake and anesthetized mice. J. Neurosci. *36*, 12144–12156.

Eckert MJ, Guévremont D, Williams JM, Abraham WC. 2013. Rapid visual stimulation increases extrasynaptic glutamate receptor expression but not visual-evoked potentials in the adult rat primary visual cortex. Eur. J. Neurosci. 37, 400–406

Fiebelkorn IC, Pinsk MA, Kastner S. 2018. A Dynamic Interplay within the Frontoparietal Network Underlies Rhythmic Spatial Attention. Neuron *99*, 842-853.e8.

Frenkel MY, Sawtell NB, Diogo AC, Yoon B, Neve RL, Bear MF. 2006. Instructive effect of visual experience in mouse visual cortex. Neuron *51*, 339–349.

Gao E, DeAngelis GC, Burkhalter A. 2010. Parallel input channels to mouse primary visual cortex. J. Neurosci. *30*, 5912–5926.

Gavornik JP, Bear MF. 2014. Learned spatiotemporal sequence recognition and prediction in primary visual cortex. Nat. Neurosci. *17*, 732–737.

Gu Y, Huang S, Chang MC, Worley P, Kirkwood A, Quinlan EM. 2013. Obligatory role for the immediate early gene NARP in critical period plasticity. Neuron *79*, 335.

Guo W, Clause AR, Barth-Maron A, Polley DB. 2017. A Corticothalamic Circuit for Dynamic Switching between Feature Detection and Discrimination. Neuron *95*, 180-194.e5.

Han F, Caporale N, Dan Y. 2008. Reverberation of Recent Visual Experience in Spontaneous Cortical Waves. Neuron *60*, 321–327.

Heynen AJ, Bear MF. 2001. Long-term potentiation of thalamocortical transmission in the adult visual cortex in vivo. J Neurosci. 21:9801–9813.

Horner AE, Heath CJ, Hvoslef-Eide M, Kent BA, Kim CH, Nilsson SRO, Alsiö J, Oomen CA, Holmes A, Saksida LM, Bussey TJ. 2013. The touchscreen operant platform for testing learning and memory in rats and mice. Nat Protoc. 8:1961–1984.

Howe, WM, Gritton HJ, Lusk NA, Roberts EA, Hetrick VL, Berke JD, Sarter M. 2017. Acetylcholine Release in Prefrontal Cortex Promotes Gamma Oscillations and Theta-Gamma Coupling during Cue Detection. J. Neurosci. *37*, 3215–3230.

Iurilli G, Ghezzi D, Olcese U, Lassi G, Nazzaro C, Tonini R, Tucci V, Benfenati F, Medini P. 2012. Sound-Driven Synaptic Inhibition in Primary Visual Cortex. Neuron *73*, 814–828.

Jutras MJ, Fries P, Buffalo EA. 2009. Gamma-band synchronization in the macaque hippocampus and memory formation. J. Neurosci. *29*, 12521–12531.

Kaplan ES, Cooke SF, Komorowski RW, Chubykin AA, Thomazeau A, Khibnik LA, Gavornik JP, Bear MF. 2016. Contrasting roles for parvalbumin-expressing inhibitory neurons in two forms of adult visual cortical plasticity. Elife *5*.

Kim YJ, Grabowecky M, Paller KA, Muthu K, Suzuki, S. 2007. Attention induces synchronization-based response gain in steady-state visual evoked potentials. Nat. Neurosci. *10*, 117–125.

Kirk IJ, McNair NA, Hamm JP, Clapp WC, Mathalon DH, Cavus I, Teyler TJ. 2010. Long- term potentiation (LTP) of human sensory- evoked potentials. Wiley Interdiscip Rev Cogn Sci. 1:766–773.

Kirkwood A, Rioult MG, Bear MF. 1996. Experience-dependent modification of synaptic plasticity in visual cortex. Nature 381, 526–528.

Kissinger ST, Pak A, Tang Y, Masmanidis SC, Chubykin, AA. 2018. Oscillatory Encoding of Visual Stimulus Familiarity. J. Neurosci. *38*, 6223–6240.

Kissinger ST, Wu Q, Quinn CJ, Anderson AK, Pak A, Chubykin AA. 2020. Visual Experience-Dependent Oscillations and Underlying Circuit Connectivity Changes Are Impaired in Fmr1 KO Mice. Cell Rep. *31*, 107486.

Larson J, Wong D, Lynch, G. 1986. Patterned stimulation at the theta frequency is optimal for the induction of hippocampal long-term potentiation. Brain Res. *368*, 347–350.

Lisman J. 2010. Working Memory: The Importance of Theta and Gamma Oscillations. Curr. Biol. *20*, R490–R492.

Mayford M, Wang J, Kandel ER, O'Dell TJ. 1995. CaMKII regulates the frequency-response function of hippocampal synapses for the production of both LTD and LTP. Cell 81, 891–904.

Marshel JH, Garrett ME, Nauhaus I, Callaway EM. 2011. Functional specialization of seven mouse visual cortical areas. Neuron *72*, 1040–1054.

Marzoll A, Saygi T, Dinse HR. 2018. The effect of LTP- and LTD-like visual stimulation on modulation of human orientation discrimination. Sci. Rep. *8*, 16156.

Mitzdorf U. 1985. Current source-density method and application in cat cerebral cortex: investigation of evoked potentials and EEG phenomena. Physiol. Rev. *65*, 37–100.

Montgomery SM, Buzsáki G. 2007. Gamma oscillations dynamically couple hippocampal CA3 and CA1 regions during memory task performance. Proc. Natl. Acad. Sci. U. S. A. *104*, 14495–14500.

Murase S, Lantz CL, Quinlan EM. 2017. Light reintroduction after dark exposure reactivates plasticity in adults via perisynaptic activation of MMP-9. Elife *6*.

Nabavi S, Fox R, Proulx CD, Lin JY, Tsien RY, Malinow R. 2014. Engineering a memory with LTD and LTP. Nature *511*, 348–352.

Niell CM, Stryker MP. 2008. Highly selective receptive fields in mouse visual cortex. J. Neurosci. *28*, 7520–7536.

Niell CM, Stryker MP. 2010. Modulation of visual responses by behavioral state in mouse visual cortex. Neuron *65*, 472–479.

O'Brien RJ, Xu D, Petralia RS, Steward O, Huganir RL, Worley P. 1999. Synaptic clustering of AMPA receptors by the extracellular immediate-early gene product Narp. Neuron *23*, 309–323.

O'Riordan KJ, Hu NW, Rowan MJ. 2018. Physiological activation of mGlu5 receptors supports the ion channel function of NMDA receptors in hippocampal LTD induction in vivo. Sci. Rep. 8, 1–12

ten Oever S, Schroeder CE, Poeppel D, Van Atteveldt N, Mehta AD, Mégevand P, Groppe DM, Zion-Golumbic E. 2017. Low-frequency cortical oscillations entrain to subthreshold rhythmic auditory stimuli. J. Neurosci. *37*, 4903–4912.

Park H, Lee DS, Kang E, Kang H, Hahm J, Kim JS, Chung CK, Jiang H, Gross J, Jensen O. 2016. Formation of visual memories controlled by gamma power phase-locked to alpha oscillations. Sci. Rep. *6*, 28092.

Pegado F, Vankrunkelsven H, Steyaert J, Boets B, De Beeck HO, Op de Beeck H. 2016. Exploring the Use of Sensorial LTP/LTD-Like Stimulation to Modulate Human Performance for Complex Visual Stimuli. PNAS *11*, e0158312.

Pelli DG. 1997. The VideoToolbox software for visual psychophysics: transforming numbers into movies. Spat. Vis. *10*, 437–442.

Poggio T, Fahle M, Edelman S, Askenasy J, Sagi D. 1992. Fast perceptual learning in visual hyperacuity. Science 80-. . *256*, 1018–1021.

Prusky GT, West PWR, Douglas RM. 2000. Behavioral assessment of visual acuity in mice and rats. Vision Res. 40:2201–2209.

Rodríguez-Durán LF, Martínez-Moreno A, Escobar ML. 2017. Bidirectional modulation of taste aversion extinction by insular cortex LTP and LTD. Neurobiol. Learn. Mem. 142, 85–90.

Ross RM, McNair NA, Fairhall SL, Clapp WC, Hamm JP, Teyler TJ, Kirk IJ. 2008. Induction of orientation-specific LTP-like changes in human visual evoked potentials by rapid sensory stimulation. Brain Res. Bull. 76, 97–101

Saleem AB, Lien AD, Krumin M, Haider B, Rosón MR, Ayaz A, Reinhold K, Busse L, Carandini M, Harris KD, Carandini M. 2017. Subcortical Source and Modulation of the Narrowband Gamma Oscillation in Mouse Visual Cortex. Neuron. 93:315–322.

Sanders PJ, Thompson B, Corballis PM, Maslin M, Searchfield GD. 2018. A review of plasticity induced by auditory and visual tetanic stimulation in humans. Eur. J. Neurosci. *48*, 2084–2097.

Sauseng P, Klimesch W, Gruber WRR, Hanslmayr S, Freunberger R, Doppelmayr M. 2007. Are event-related potential components generated by phase resetting of brain oscillations? A critical discussion. Neuroscience 146, 1435–1444.

Schroeder CE, Lakatos P. 2009. Low-frequency neuronal oscillations as instruments of sensory selection. Trends Neurosci. 32, 9–18

Sohal VS, Zhang F, Yizhar O, Deisseroth K. 2009. Parvalbumin neurons and gamma rhythms enhance cortical circuit performance. Nature *459*, 698–702.

Stark E, Eichler R, Roux L, Fujisawa S, Rotstein HG, Buzsáki G. 2013. Inhibition-Induced theta resonance in

cortical circuits. Neuron *80*, 1263–1276.

Stringer C, Pachitariu M, Steinmetz N, Reddy CB, Carandini M, Harris, KD. 2019. Spontaneous behaviors drive multidimensional, brainwide activity. Science *364*, 255.

Sumner RL, Spriggs MJ, Muthukumaraswamy SD, Kirk IJ. 2020. The role of Hebbian learning in human perception: a methodological and theoretical review of the human Visual Long-Term Potentiation paradigm. Neurosci Biobehav Rev.

Tanimoto N, Sothilingam V, Kondo M, Biel M, Humphries P, Seeliger MW. 2015. Electroretinographic assessment of rod- and cone-mediated bipolar cell pathways using flicker stimuli in mice. Sci. Rep. *5*, 10731.

Teyler TJ, Hamm JP, Clapp WC, Johnson BW, Corballis MC, Kirk IJ. 2005. Long-term potentiation of human visual evoked responses. Eur. J. Neurosci. 21, 2045–2050.

Veit J, Hakim R, Jadi MP, Sejnowski TJ, Adesnik H. 2017. Cortical gamma band synchronization through somatostatin interneurons. Nat. Neurosci. *20*, 951–959.

Williams J. 2001. Frequency-specific effects of flicker on recognition memory. Neuroscience *104*, 283–286.

Williams J, Ramaswamy D, Oulhaj A. 2006. 10 Hz flicker improves recognition memory in older people. BMC Neurosci. *7*, 21.

Xing D, Yeh CI, Burns S, Shapley RM. 2012. Laminar analysis of visually evoked activity in the primary visual cortex. Proc. Natl. Acad. Sci. U. S. A. *109*, 13871–13876.

Xu D, Hopf C, Reddy R, Cho RW, Guo L, Lanahan A, Petralia RS, Wenthold RJ, O'Brien RJ, Worley, P. 2003. Narp and NP1 Form Heterocomplexes that Function in Developmental and Activity-Dependent Synaptic Plasticity. Neuron *39*, 513–528.

Zaehle T, Clapp WC, Hamm JP, Meyer M, Kirk IJ. 2007. Induction of LTP-like changes in human auditory cortex by rapid auditory stimulation: An FMRI study. Restor. Neurol. Neurosci. *25*, 251–259.

Zhang LI, Tao HZW, Poo MM. 2000. Visual input induces long-term potentiation of developing retinotectal synapses. Nat. Neurosci. 3, 708–715.

Zold CL, Hussain Shuler MG. 2015. Theta Oscillations in Visual Cortex Emerge with Experience to Convey Expected Reward Time and Experienced Reward Rate. J. Neurosci. *35*, 9603–9614.

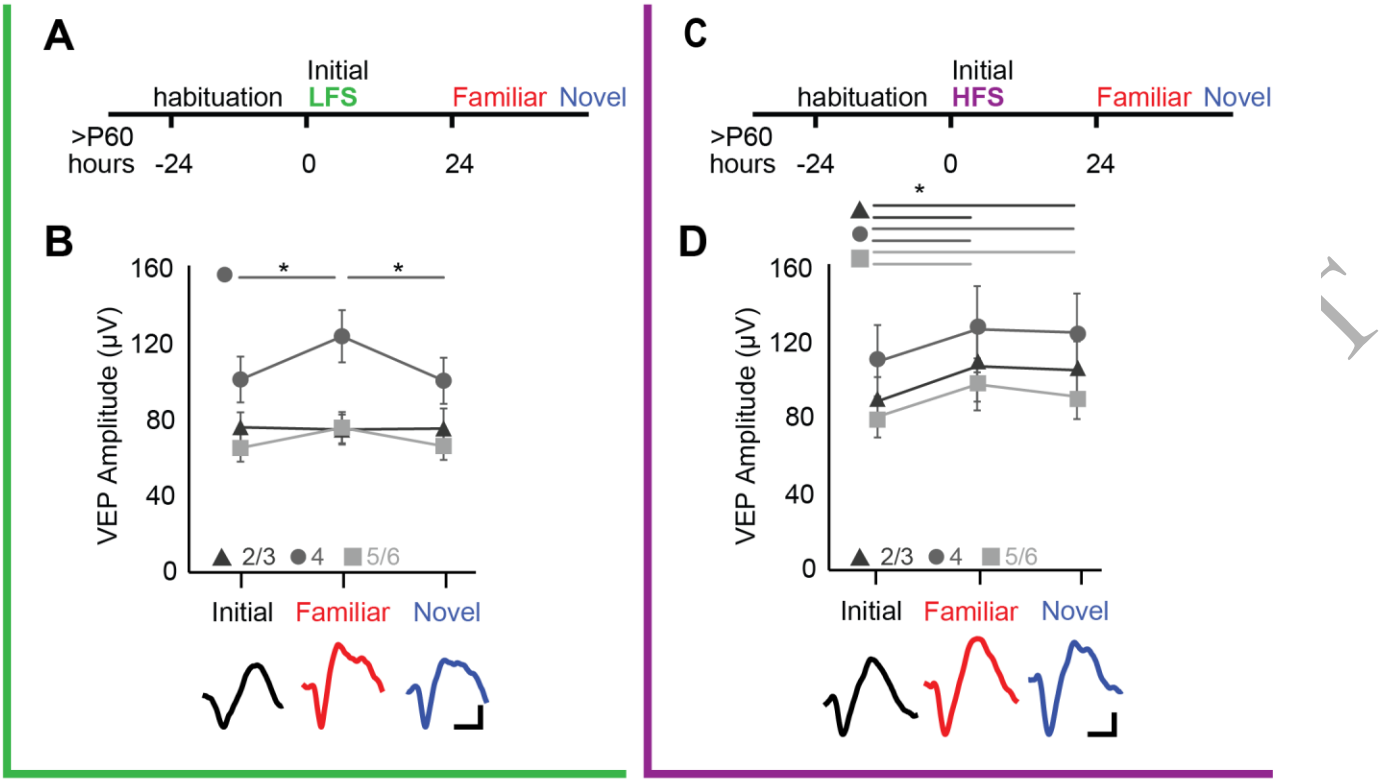


**Figure 1. LFS and HFS differentially impact the location and generalization of visual response potentiation.** A) Experimental timeline: naïve adult subjects (>P60) received low frequency visual stimulation (LFS, green: 200 presentations of 0.05 cpd, 100% contrast gratings, 60° orientation, 2 Hz). The initial response is reported as baseline VEP. After 24 hours, VEPs were evoked by visual stimuli with familiar and novel orientations presented at 2 Hz. B) Significant increase in VEP amplitude in layer 4 (circles) in response to familiar, but not novel, stimuli (RANOVA $_{(df, 2, 15)}$, $F = 9.13$, $p < 0.001$; * = Bonferroni *post hoc* $p < 0.05$; n=16 subjects). Bottom: representative example of layer 4 VEP in response to initial (black) familiar (red) and novel (blue) stimuli. Cal = 20 μV, 50 ms C) Timeline, as in A, except that naïve adult subjects received high frequency visual stimulation (HFS, purple: 200 presentations of 0.05 cycle per degree, 100% contrast grating, 30° orientation, 20 Hz) after initial assessment of baseline VEP. After 24 hours, VEPs were evoked by visual stimuli with familiar and novel orientations presented at 2 Hz. D) Significant increase in VEP amplitudes in layers 2/3 (triangles), 4 (circles), and 5/6 (squares) in response to familiar and novel stimuli (RANOVA $_{(df, 2, 10)}$, layer 2/3: $F = 5.25$, $p = 0.015$, layer 4: $F = 7.31$, $p = 0.004$; layer 5/6: $F = 11.41$, $p < 0.001$; * = Bonferroni *post hoc* $p<0.05$; n = 11 subjects). Bottom: representative example of layer 4 VEP in response to initial (black) familiar (red) and novel (blue) stimuli. Cal = 20 μV, 50 ms.

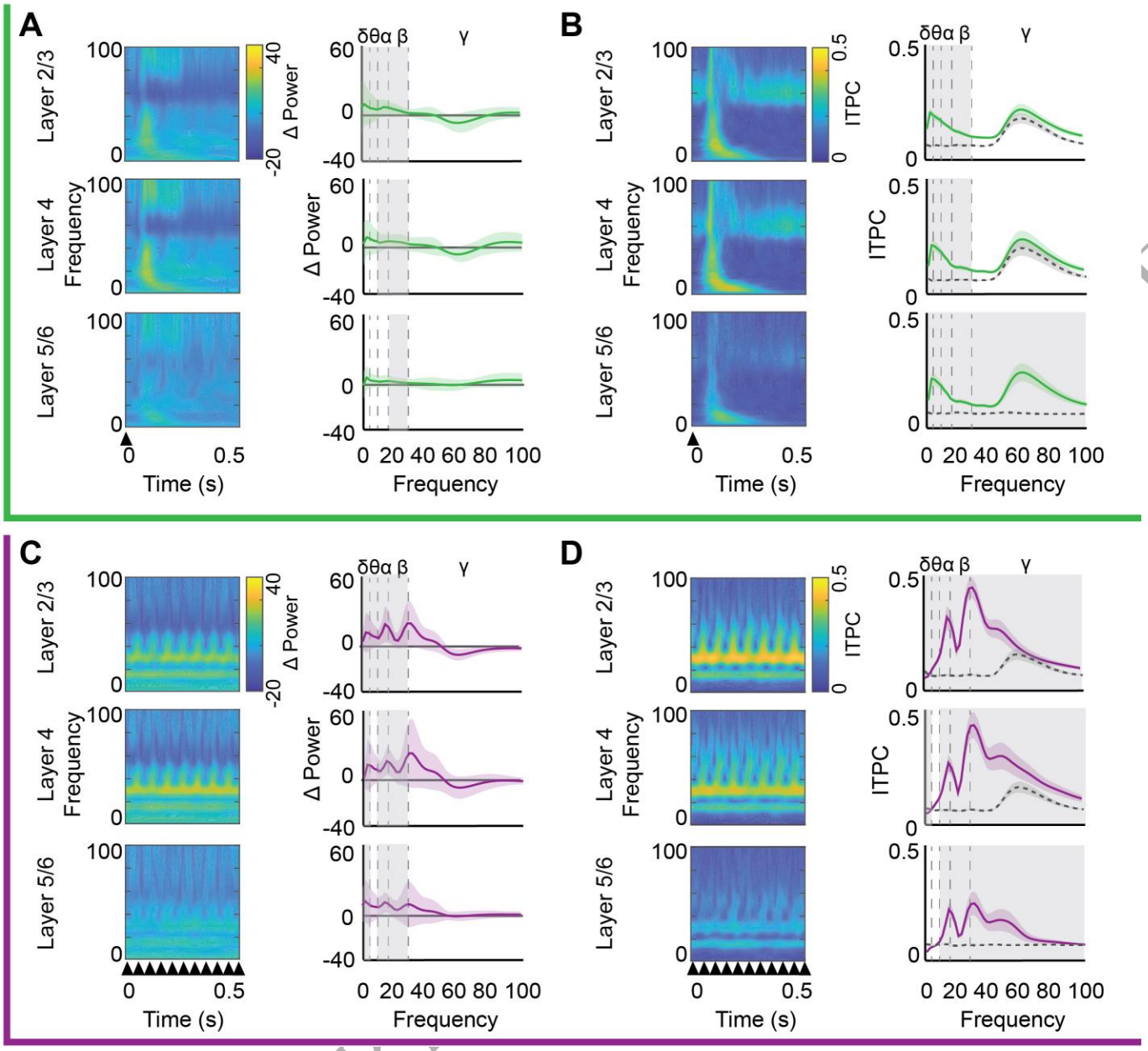


**Figure 2. Distinct acute impact of LFS and HFS on oscillatory power and evoked phase reset.** Top, green, during LFS: A) Left; average oscillatory power (heat map) from 0-100 Hz (3 Hz bins; y axis) over time (x axis) by cortical layer during LFS. Power was normalized to spontaneous activity in response to 26 cd/m$^2$ grey screen. Right; significant increase in average α and β power across all cortical layers, δ power in layers 2/3 and 4, and θ power in layers 2/3 and 5/6 during LFS (One sample t-test, Grey highlight = $p < 0.05$, n = 16). Power binned by frequency band (δ: 1-4, θ: 4-8, α: 8-13, β: 13-30, γ: 30-100Hz). B) Left; average inter-trial phase consistency during LFS (ITPC; heat map) from 0-100 Hz (in 3 Hz bins; y axis) over time (x axis), trial averaged. Right; a significant increase in ITPC for all frequencies in layer 2/3 ($MANOVA_{(df, 1, 5)}$, $F = 15.94$, $p < 0.001$), and all frequencies below gamma in layers 4 ($MANOVA_{(df, 1, 15)}$, $F = 15.98$, $p < 0.001$) and 5/6 ($MANOVA_{(df, 1, 15)}$, $F = 11.10$, $p < 0.001$) during LFS (solid line), relative to spontaneous activity (dashed line). Grey highlight = Bonferroni *post hoc* $p < 0.05$; n = 16 subjects. Bottom, purple, during HFS: C) Left; average

oscillatory power (heat map) from 0-100 Hz (3 Hz bins; y axis) over time (x axis) by cortical layer during HFS, normalized as in A. Right; A significant increase in average δ, α and β power in all cortical layers and in θ power in layer 2/3 during HFS (one sample t-test, Grey highlight = $p < 0.05$, n = 11). D) Left; average inter-trial phase consistency during HFS (ITPC; heat map) from 0-100 Hz (in 3 Hz bins; y axis) over time (x axis), trial averaged as in B. Right; Significant changes in ITPC in all cortical layers, including a significant increase in visually driven phase reset in α, and β oscillations (layer 2/3: $MANOVA_{(df, 1, 10)}$, $F = 14.14$, $p < 0.001$, layer 4: $MANOVA_{(df, 1, 10)}$, $F = 12.284$, $p < 0.001$, layer 5: $MANOVA_{(df, 1, 10)}$, $F = 9.95$, $p = 0.0017$), and a significant decrease in the δ oscillation in all layers, during HFS (purple) relative to spontaneous activity (dashed line). Grey highlight = Bonferroni *post hoc* $p < 0.05$; n = 11 subjects. Stimulus onset denoted by arrowheads.

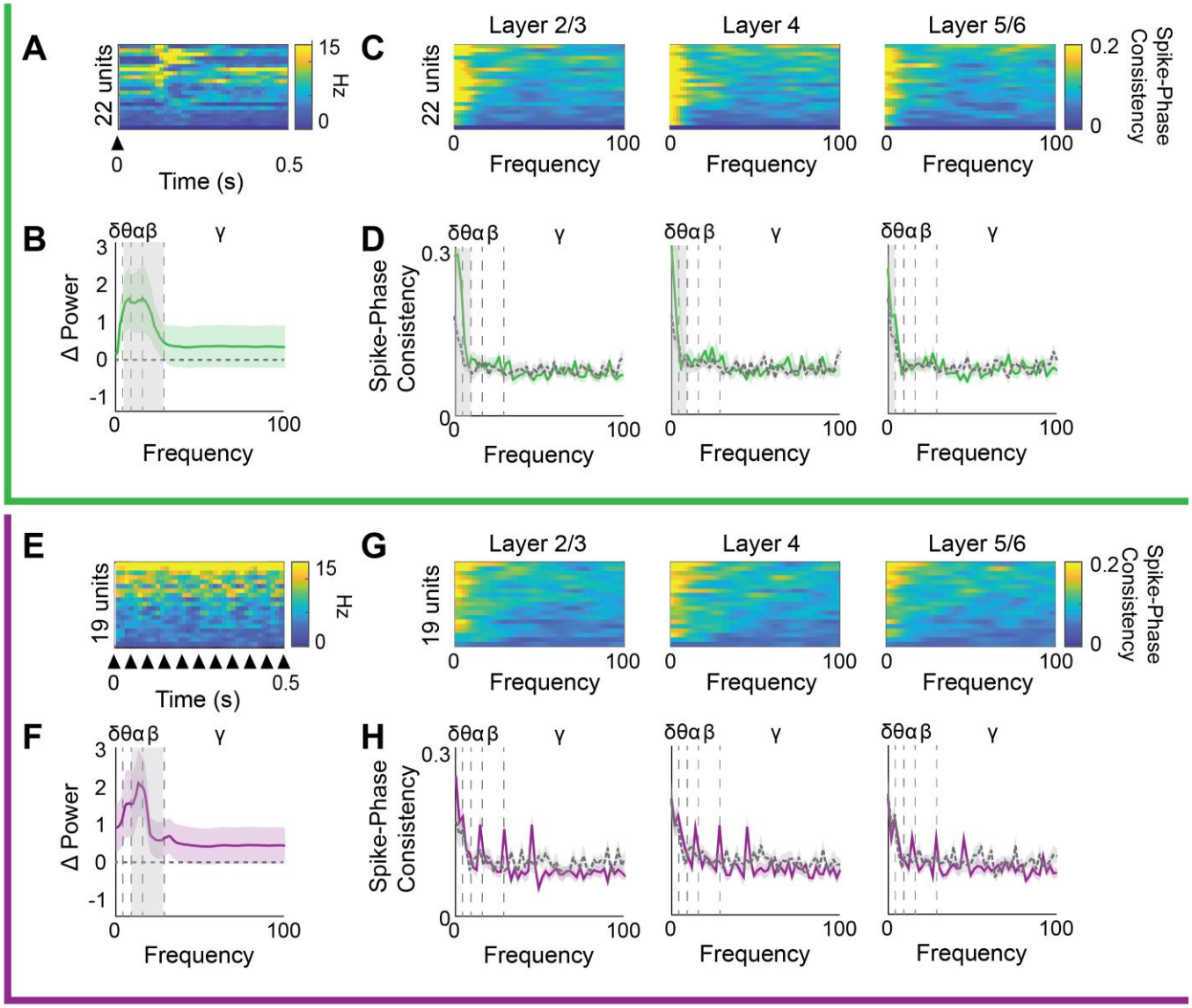


**Figure 3. Distinct acute impact of LFS and HFS on FS IN oscillatory power and LFP phase synchrony.** Top, green, during LFS: A) Heat map depicting PSTH for each FS IN. B) Average change in oscillatory power of FS INs during LFS, binned by frequency band (δ: 1-4, θ: 4-8, α: 8-13, β: 13-30, γ: 30-100Hz, n = 16

subjects). A significant increase in the power of θ, α, and β oscillations in FS IN during LFS (One sample t-test with Bonferroni correction, grey highlight = p<0.05). C) Heat map of FS IN spike-LFP phase consistency during LFS for each FS IN compared to LFP of each layer. D) FS IN spike-LFP phase consistency during LFS (green) compared to spontaneous activity (grey), by frequency (average +/- SEM). LFS increases FS IN spike-phase consistency with δ oscillations in all cortical layers and with θ in layers 2/3 and 4 (Two-sample t-test, grey highlight = $p < 0.05$, n = 16 subjects). Bottom, purple, during HSF: E) Heat map depicting PSTH for each FS IN. F) Average change in oscillatory power of FS IN spiking during HFS, power binned by frequency band (δ 1-4, θ: 4-8, α: 8-13, β: 13-30, γ: 30-100Hz, n = 11 subjects). A significant increase in the power of α and β oscillations in FS INs during HFS (One sample t-test, with Bonferroni correction, grey highlight = $p < 0.05$). G) Heat map of FS IN spike-LFP phase consistency during HFS for each FS IN compared to LFP of each layer. H) Average +/- SEM FS INs spike-LFP phase consistency during HFS (purple) compared to spontaneous (grey) by frequency. HFS does not change FS IN spike-phase consistency in any cortical layer (n = 11 subjects).

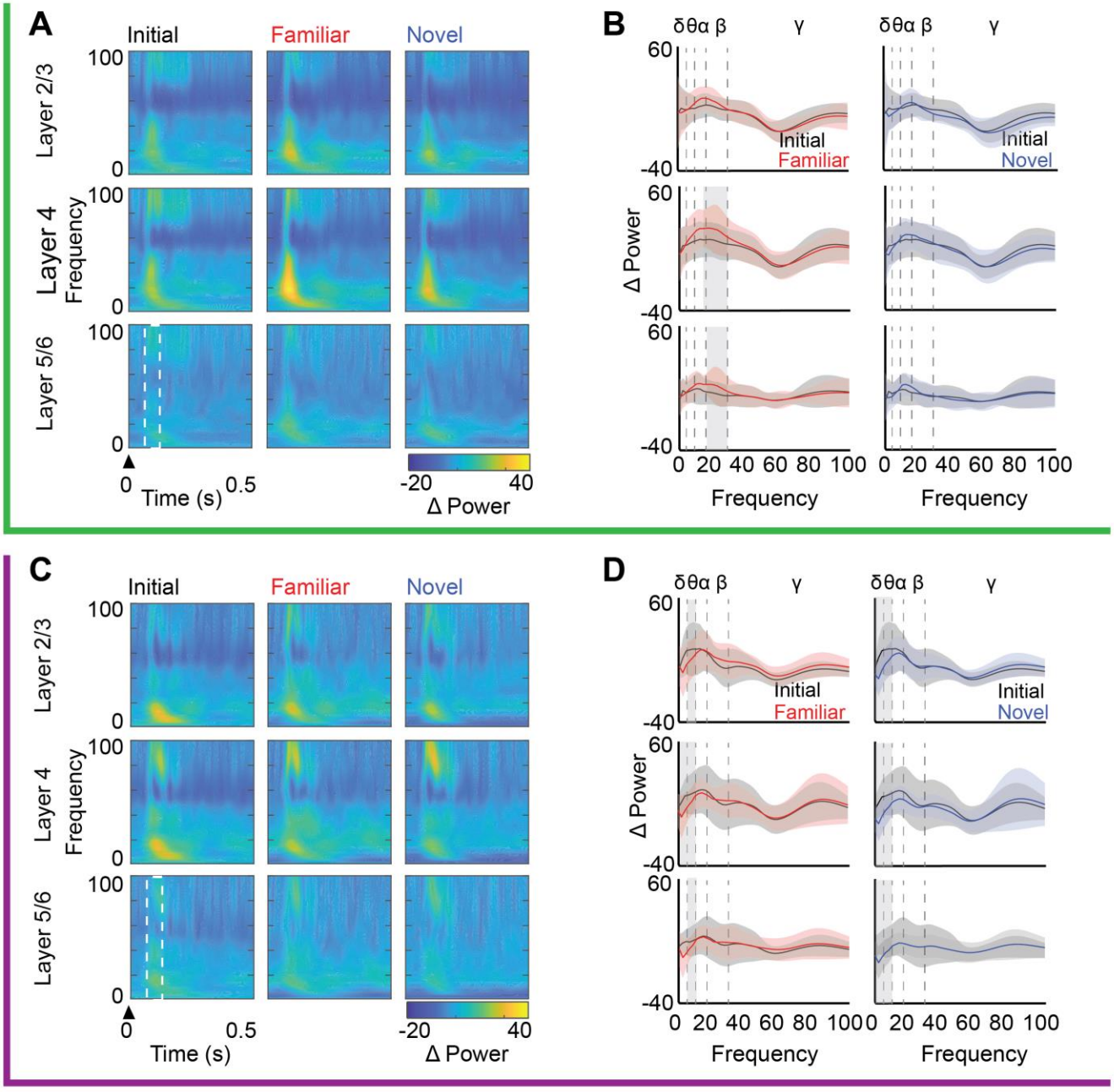


**Figure 4. LFS and HFS differentially impact oscillatory power during subsequent visual stimulation.** Top, green, after LFS: A) Left; average oscillatory power (heat map) from 0 –100 Hz (3 Hz bins; y axis) over time (x axis) by cortical layer during initial LFS, and in response to familiar and novel visual stimuli 24 hours after LFS. Power is normalized to pre-experimental spontaneous activity acquired during viewing of a 26 cd/m$^2$ grey screen. Arrowhead indicates stimulus onset, white box indicates time window for assessment of change in oscillatory power (100-200 ms after stimulus onset). B) Change in oscillatory power (average +/- SEM), binned by frequency band (δ: 1-4, θ: 4-8, α: 8-13, β: 13-30, γ: 30-100 Hz) during presentation of initial (black), familiar (red), and novel (blue) visual stimuli. In layers 4 and 5/6, a significant increase in average β power in response to familiar (red) but not novel (blue) visual stimuli relative to initial, in subjects that received LFS (black, RANOVA $_{(df, 2, 15)}$, layer 4: F = 6.51, p = 0.004; layer 5/6: F = 3.92, p = 0.031). Grey highlight = Bonferroni *post*

*hoc* p < 0.05; n = 16 subjects. Bottom, purple, after HFS: C) Average oscillatory power (heat map) from 0-100 Hz (3Hz bins; y axis) over time (x axis) by cortical layer during initial HFS, and in response to presentation of familiar and novel visual stimulus orientations 24 hours after HFS. Power was normalized as in A. Arrowhead indicates stimulus onset, white box indicates time window for assessment of change in oscillatory power (100-200 ms after stimulus reversal). D) Change in oscillatory power (average +/- SEM), binned by frequency band during presentation of initial (black), familiar (red), and novel (blue) visual stimuli. A decrease in average θ power in response to novel (blue) and familiar (red) visual stimuli, in all layers in subjects that received HFS (RANOVA $_{(df, 2, 10)}$, layer 2/3: F = 8.63, p = 0.002, layer 4: F = 8.47, p = 0.002, layer 5: F = 7.936, p = 0.003). Grey highlight = Bonferroni *post hoc* p < 0.05; n = 11 subjects.

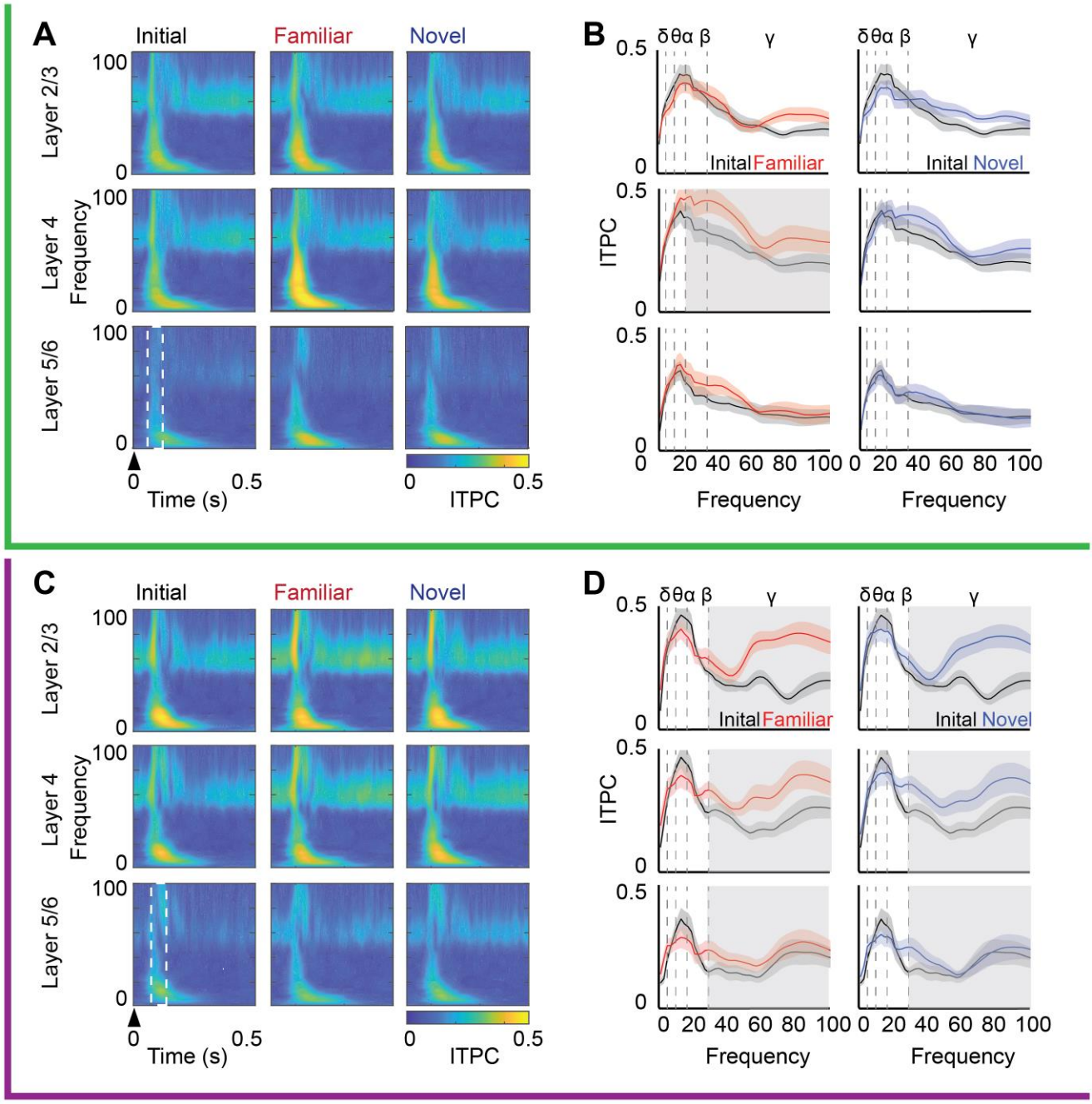

**Figure 5. ITPC co-varies with LFS and HFS-induced visual response potentiation.** Top, green, after LFS: A) Average inter-trial phase consistency 24 hours after LFS in response familiar and novel visual stimuli compared to initial response (ITPC; heat map) from 0-100 Hz (in 3 Hz bins; y axis) over time (x axis). Trial averaged from complex Morlet wavelet convolution. Arrowhead indicates stimulus onset; white box indicates time window for assessment of change in ITPC (100-200 ms after stimulus onset). B) Average ITPC power binned by frequency band (δ: 1-4, θ: 4-8, α: 8-13, β: 13-30, γ: 30-100Hz) in response to initial (black), familiar (red), and novel (blue) visual stimuli. 24 hours after LFS, the familiar visual stimulus induced a significant increase phase reset of β and γ oscillations in layer 4 relative to initial response (black, RANOVA $_{(df, 2, 15)}$, β: $F = 5.20$, $p = 0.011$, γ: $F = 8.82$, $p < 0.001$). Grey highlight = Bonferroni *post hoc* $p < 0.05$; n = 16 subjects. Bottom, purple, after HFS: C) Average ITPC 24 hours after HFS in response to familiar and novel visual stimuli, compared to initial response (ITPC; heat map) from 0-100 Hz (in 3 Hz bins; y axis) over time (x axis). Trial averaged from complex Morlet wavelet convolution. Arrowhead indicates stimulus onset; white box indicates time window for assessment of change in ITPC (100-200 ms after stimulus reversal). D) Average ITPC power binned by frequency band (δ: 1-4, θ: 4-8, α: 8-13, β: 13-30, γ: 30-100Hz) in response to initial (black), familiar (red), and novel (blue) visual stimuli. 24 hours after HFS, familiar (red) and novel (blue) visual stimuli induced a significant increase in phase reset of γ oscillations in all cortical layers relative to initial (black, RANOVA $_{(df, 2, 10)}$, layer 2/3: $F = 19.42$, $p < 0.001$, layer 4: $F = 13.04$, $p < 0.001$, layer 5: $F = 5.29$, $p = 0.025$). Grey highlight = Bonferroni *post hoc* $p < 0.05$; n = 11 subjects.

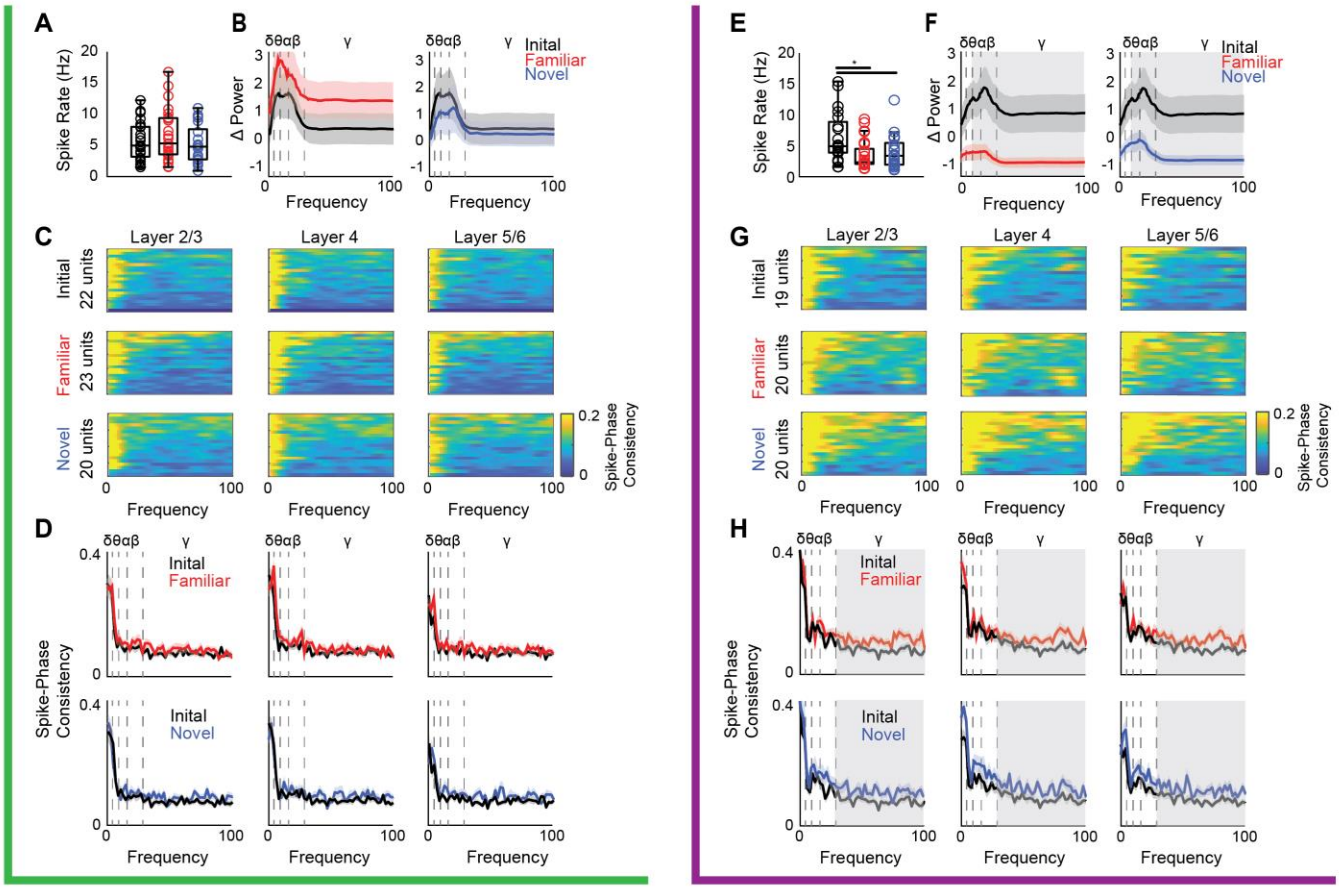

**Figure 6. HFS decreases FS IN firing rates and power and increases FS IN spike-LFP gamma phase consistency.** Top, green, after LFS: A) No change in average spike rates of FS IN during presentation of familiar or novel visual stimuli 24 hours after LFS. B) No change in FS IN oscillatory power during presentation of familiar (red, top) or novel (blue, bottom) visual stimuli relative to initial (black). C) Heat map of spike-phase consistency of FS INs during initial LFS, and familiar and novel visual stimuli 24 hours after LFS by cortical layer from 0 - 100 Hz during the 100-200 ms following stimulus onset. D) Average FS IN-LFP spike-phase consistency by cortical layer in response to initial (black), familiar (red), and novel (blue) stimuli. No significant difference in spike-phase consistency 24 hours after LFS. Bottom, purple, after HFS: E) 24 hours after HFS, visual stimuli with familiar (red) and novel (blue) orientations significantly decreased average FS IN spike rate ($ANOVA_{(df, 2, 56)}$, $F = 4.50$, $p = 0.015$). * = Tukey *post hoc* $p < 0.05$; n = 11 subjects. F) Average change in FS IN oscillatory power by frequency during initial HFS (black) and familiar (red) and novel (blue) visual stimuli 24 hours after HFS. A significant decrease in the oscillatory power of FS IN across multiple frequencies (7-100Hz) during familiar and novel stimuli compared to initial (black; $ANOVA_{(df, 2, 56)}$, α: $F = 6.862$, $p = 0.002$, β: $F = 8.898$, $p = 0.0004$, γ: $F = 5.998$, $p = 0.004$). Grey highlight = Bonferroni *post hoc* $p < 0.05$, n = 11 subjects. G) Heat map of spike- phase consistency of FS IN during initial HFS, and familiar and novel visual stimuli 24 hours after HFS by cortical layer from 0-100 Hz during the 100-200 ms following stimulus reversal. H) Average FS IN spike-LFP phase consistency by cortical layer induced by initial (black), familiar (red), and novel (blue) stimuli. 24 hours after HFS, familiar and novel visual stimuli induced a significant increase in FS IN spike-LFP γ phase consistency in all cortical layers ($ANOVA_{(df, 2, 56)}$, Layer 2/3: $F = 6.795$, $p = 0.002$, layer 4: $F = 5.655$, $p = 0.006$, layer 5: $F = 6.072$, $p = 0.004$). Grey highlight = Bonferroni *post hoc* $p < 0.05$; n = 11 subjects.

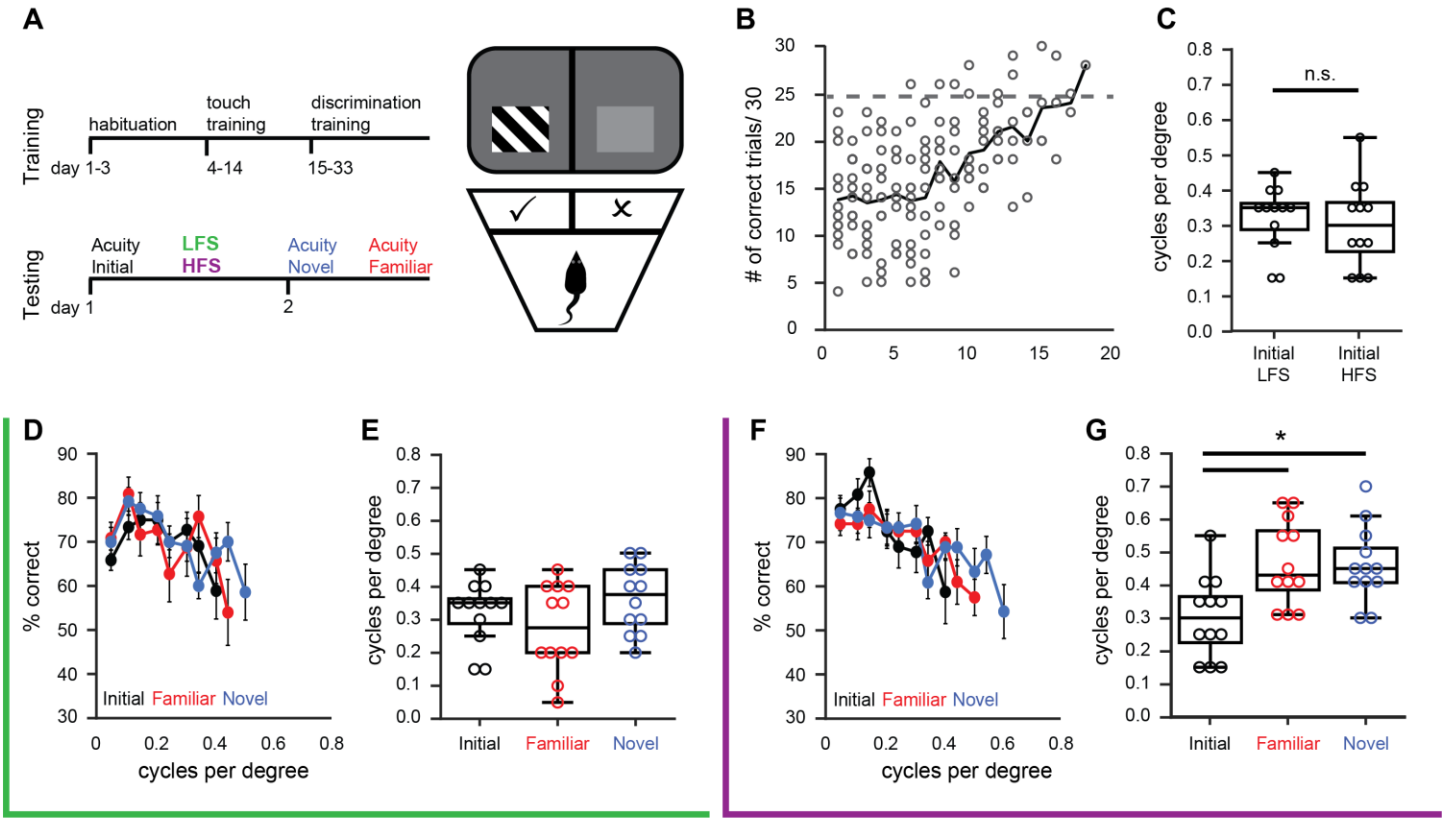


**Figure 7. HFS enhances visual acuity.** A) Left: timeline, subjects were trained in a 2-alternative forced choice visual detection task until they reached criterion of 25/30 correct choices at 0.05 cpd. Baseline visual acuity was assessed using a novel stimulus orientation and followed by LFS or HFS. Spatial acuity was tested again 24 hours after LFS or HFS. Right: cartoon depicting modified Bussey chamber with plexiglass divider to define the choice point for the determination of stimulus spatial frequency. B) All subjects reached task criterion by 18 days of training. C) No significant difference in initial visual acuity prior to the delivery of LFS or HFS (Student's t-test, p = 0.63). D) Average frequency of seeing curves for subjects that received LFS (green box). E) No significant difference in spatial acuity probed with initial (black, before LFS), novel (blue, after LFS) and familiar (red, after LFS) visual stimulus orientations (n = 12). F) Average frequency of seeing curves for subjects that received HFS (purple box). G) A significant increase in spatial acuity probed with novel (blue, after HFS) and familiar (red, after HFS) visual stimulus orientations following HFS (black, before HFS; RANOVA $_{(df, 2, 11)}$, F = 6.817, p = 0.005). * = Bonferroni *post hoc* p < 0.05; n = 12.